Article

Cell Reports

Persistent Alterations in Microglial Enhancers in a Model of Chronic Pain

Graphical Abstract

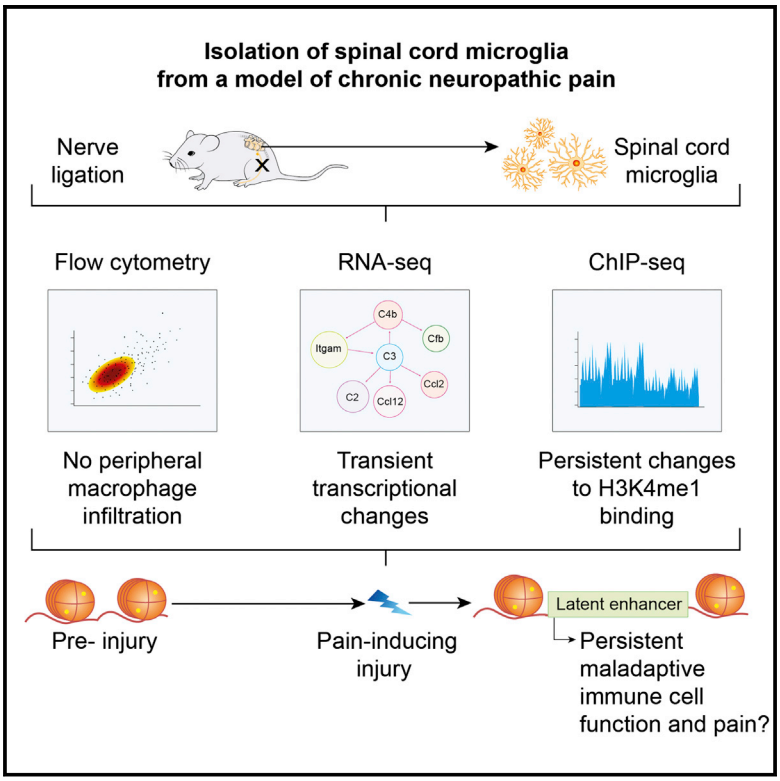

Highlights

- We examined the spinal cord immune response in a model of neuropathic pain
- No infiltration of peripheral macrophages could be detected
- RNA-seq of isolated microglia revealed a transient transcriptional response
- ChIP-seq revealed persistent, injury-induced alterations of microglial enhancers

Authors

Franziska Denk, Megan Crow, Athanasios Didangelos, Douglas M. Lopes, Stephen B. McMahon

Correspondence

franziska.denk@kcl.ac.uk (F.D.), stephen.mcmahon@kcl.ac.uk (S.B.M.)

In Brief

Chronic pain is a devastating condition, the longevity of which is not well understood. Denk et al. examined cell-type-specific microglial responses in a model of chronic pain and propose that some of the longer lasting changes from pain inducing injury may be hidden in the epigenome of these immune cells.

Accession Numbers

GSE71136
GSE71133
GSE71134

Denk et al., 2016, Cell Reports *15*, 1–11
May 24, 2016
http://dx.doi.org/10.1016/j.celrep.2016.04.063

CellPress

Please cite this article in press as: Denk et al., Persistent Alterations in Microglial Enhancers in a Model of Chronic Pain, Cell Reports (2016), http://dx.doi.org/10.1016/j.celrep.2016.04.063

Cell Reports
Article

Persistent Alterations in Microglial Enhancers in a Model of Chronic Pain

Franziska Denk,[1,*] Megan Crow,[2] Athanasios Didangelos,[1] Douglas M. Lopes,[1] and Stephen B. McMahon[1,*]
[1]Wolfson Centre for Age-Related Diseases, King's College London, London SE1 1UL, UK
[2]Stanley Institute for Cognitive Genomics, Cold Spring Harbor Laboratory, Woodbury, NY 11797, USA
*Correspondence: franziska.denk@kcl.ac.uk (F.D.), stephen.mcmahon@kcl.ac.uk (S.B.M.)
http://dx.doi.org/10.1016/j.celrep.2016.04.063

SUMMARY

Chronic pain is a common and devastating condition that induces well-characterized changes in neurons and microglia. One major unanswered question is why these changes should persist long after the precipitating injury has healed. Here, we suggest that some of the longer-lasting consequences of nerve injury may be hidden in the epigenome. Cell sorting and sequencing techniques were used to characterize the spinal cord immune response in a mouse model of chronic neuropathic pain. Infiltration of peripheral myeloid cells was found to be absent, and RNA sequencing (RNA-seq) of central microglia revealed transient gene expression changes in response to nerve ligation. Conversely, examination of microglial enhancers revealed persistent, post-injury alterations in close proximity to transcriptionally regulated genes. Enhancers are regions of open chromatin that define a cell's transcription factor binding profile. We hypothesize that changes at enhancers may constitute a mechanism by which painful experiences are recorded at a molecular level.

INTRODUCTION

All of us are likely to know someone who is affected by chronic pain: the incidence in our population is estimated to be up to 20%. With limited treatment options, many patients have long resigned and suffer quietly with little hope of respite. The hours of work and productivity they lose as a consequence turn their private tragedy into a public burden, costing the United States government an estimated $250 billion a year.

A great deal is known about the neurobiological mechanisms associated with the development and maintenance of chronic pain. One major characteristic is persistent hypersensitivity at all levels of the nervous system, with inappropriate neuronal responses having been reported in peripheral sensory neurons, spinal neurons, and top-down modulatory centers in the brain. This maladaptive state is thought to be compounded by abnormal immune cell function, both peripherally and centrally (McMahon et al., 2015). Activation of microglia in particular, the resident myeloid cells of the CNS, is known to be critical for the emergence of spinal hypersensitivity in a wide range of animal models, including those of neuropathic pain, chemotherapy-induced pain, and rheumatoid arthritis pain. Evidence in humans has been harder to come by, but pioneering imaging studies are suggesting that abnormal microglial responses also have a prominent role in the CNS of chronic pain patients (Loggia et al., 2015).

One mystery that remains is why many of these alterations persist long-term, even when the initial injury or disease remits. There are likely to be a number of explanations, for instance post-translational modification of ion channels or wide-spread transcriptional changes are often put forward. And yet, the vast majority of proteins in the brain have a half-life of <14 days (Chee and Dahl, 1978), making it difficult to appreciate how their abnormal function should be sustained in the long run. Here, we examine the possibility of epigenetic remodeling in CNS immune cells, in particular the role of enhancer deposition.

Enhancers are *cis*-acting regulatory regions within the DNA that allow the binding of multiple transcription factors (TFs) to influence gene expression over variable distances, sometimes up to several hundred kilobases (kb) away. During development, the binding of lineage-specific TFs to distinct enhancers is thought to be vital for the establishment of cell-type-specific transcription by allowing local remodeling of chromatin and permanent accessibility to selective stretches of DNA. Enhancers, therefore, ultimately determine which genes can be used in a given cell type (Heinz et al., 2015). It is thought that the enhancer profile of a cell remains largely unaltered once established. Yet recent seminal papers suggest that a small, but significant, number of de novo enhancers can appear as a result of external signals, even once development is complete. Thus in macrophages, stimulation with different inflammatory mediators or activation of toll-like receptor 4 each result in the emergence of a distinct profile of new, so-called latent, enhancer peaks (Kaikkonen et al., 2013; Ostuni et al., 2013). Some of these latent enhancers persist once the initial stimulation has been removed, in effect functioning as a molecular footprint of prior events. It has been posited that these latent enhancers could constitute a mechanism by which an adaptive form of immunity can be established in innate immune cells (Quintin et al., 2014).

We have tested this idea in context of persistent pain. We performed detailed characterization of the spinal cord immune response in a well-studied model of neuropathic pain using microglial-specific flow cytometry markers. We then isolated resident microglia for genome-wide RNA-sequencing (RNA-seq)

Please cite this article in press as: Denk et al., Persistent Alterations in Microglial Enhancers in a Model of Chronic Pain, Cell Reports (2016), http://dx.doi.org/10.1016/j.celrep.2016.04.063

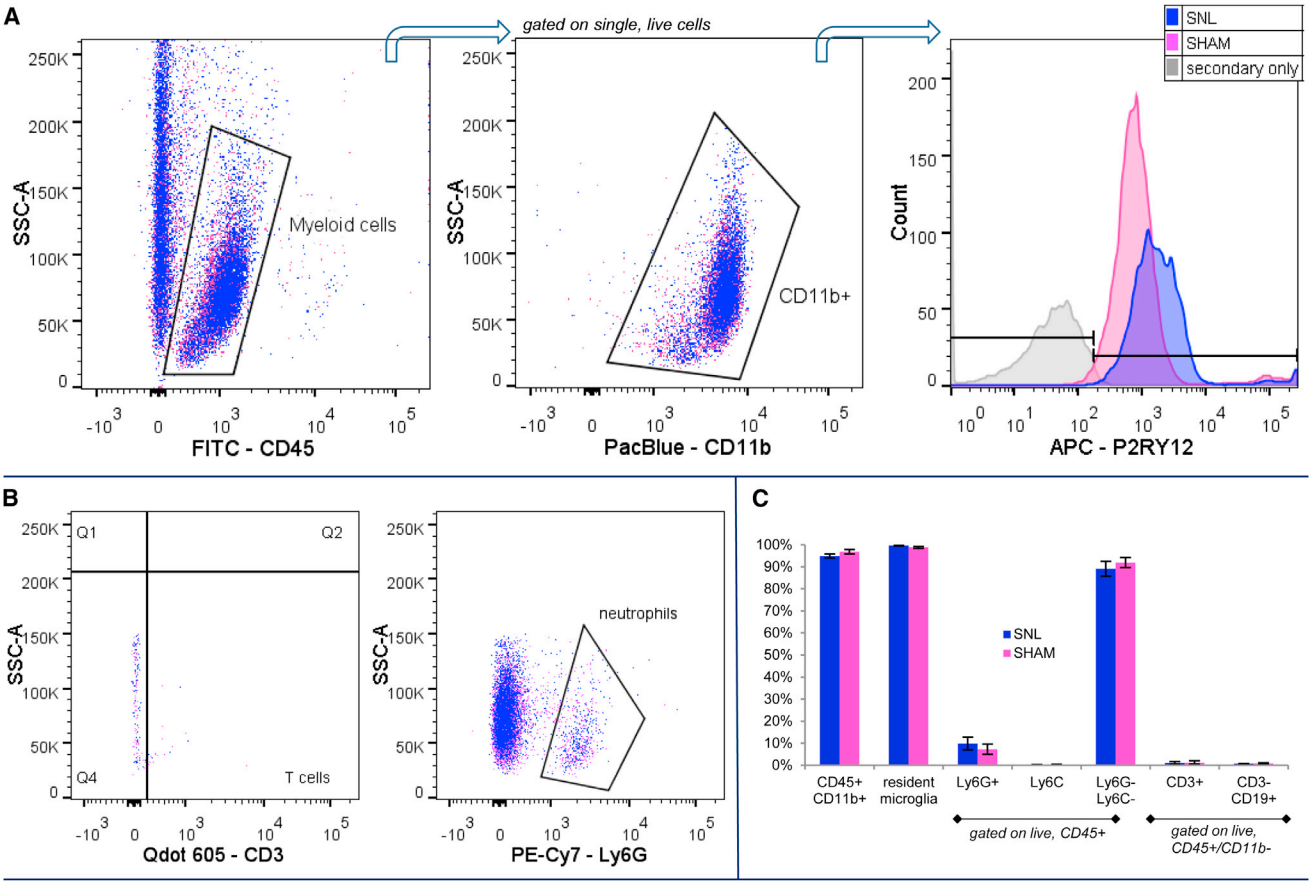

Figure 1. SNL Does Not Induce Infiltration of Peripheral Macrophages

Spinal cord microglia were acutely isolated using a Percoll gradient and analyzed via flow cytometry.

(A and B) Representative dot plots illustrating the gating strategy.

(C) No significant differences were found in cell number between sham and SNL mice for any of the markers examined: P2RY12 (resident microglia); CD3 (T cells); CD19 (B cells); Ly6G (neutrophils); Ly6C (infiltrating macrophages). Biological n = 3. Mean frequencies and SE.

See also Figure S1 and Table S1.

and epigenetic profiling. Our data provide evidence that peripheral nerve injury changes the landscape of microglial enhancers—a process that could maintain these cells in an abnormal, maladaptive state over long periods of time.

RESULTS

Characterization of Spinal Cord Immune Response after Spinal Nerve Ligation

Enhancers are highly cell-type-specific, and their study requires a firm understanding of the different cell populations present in a given system. A long-standing debate in the study of chronic pain is whether the spinal cord immune response is restricted to resident microglia or also includes peripheral macrophages. Hitherto, this question has been difficult to resolve, as common flow cytometry markers are unable to clearly distinguish between these two myeloid populations. We used a recently described antibody to unequivocally stain and identify yolk-sack-derived resident microglial populations (Butovsky et al., 2014). We also studied the proportion of other immune cells in the spinal cord, by examining Ly6G-, Ly6C-, CD3-, and CD19-positive populations to identify neutrophils, infiltrating macrophages, T cells, and B cells, respectively. There was no significant infiltration of any of these cell types into the spinal cord 7 days after partial sciatic nerve ligation (SNL) (Figure 1). The vast majority of Percoll-isolated cells were CD45-positive immune cells (92%–99%), and 98%–99% of those were resident microglia (n = 3, independent samples t test, n.s., non significant; Figure 1A). Moreover, we only found very modest numbers of neutrophils, T cells, and B cells, and their counts did not vary with injury (Figures 1B and 1C).

Enhancers can be detected via chromatin immunoprecipitation (ChIP), a technique that currently requires at least tens of thousands of cells. We therefore investigated whether Percoll isolation, with its 98%–99% resident microglial yield, would be sufficiently pure to allow for subsequent ChIP sequencing (ChIP-seq) analysis. We used an antibody to probe for a specific chromatin modification—the presence of a single methyl group at lysine residue four of histone three (H3k4me1)—that can be used as a proxy measure for enhancer location (Heintzman

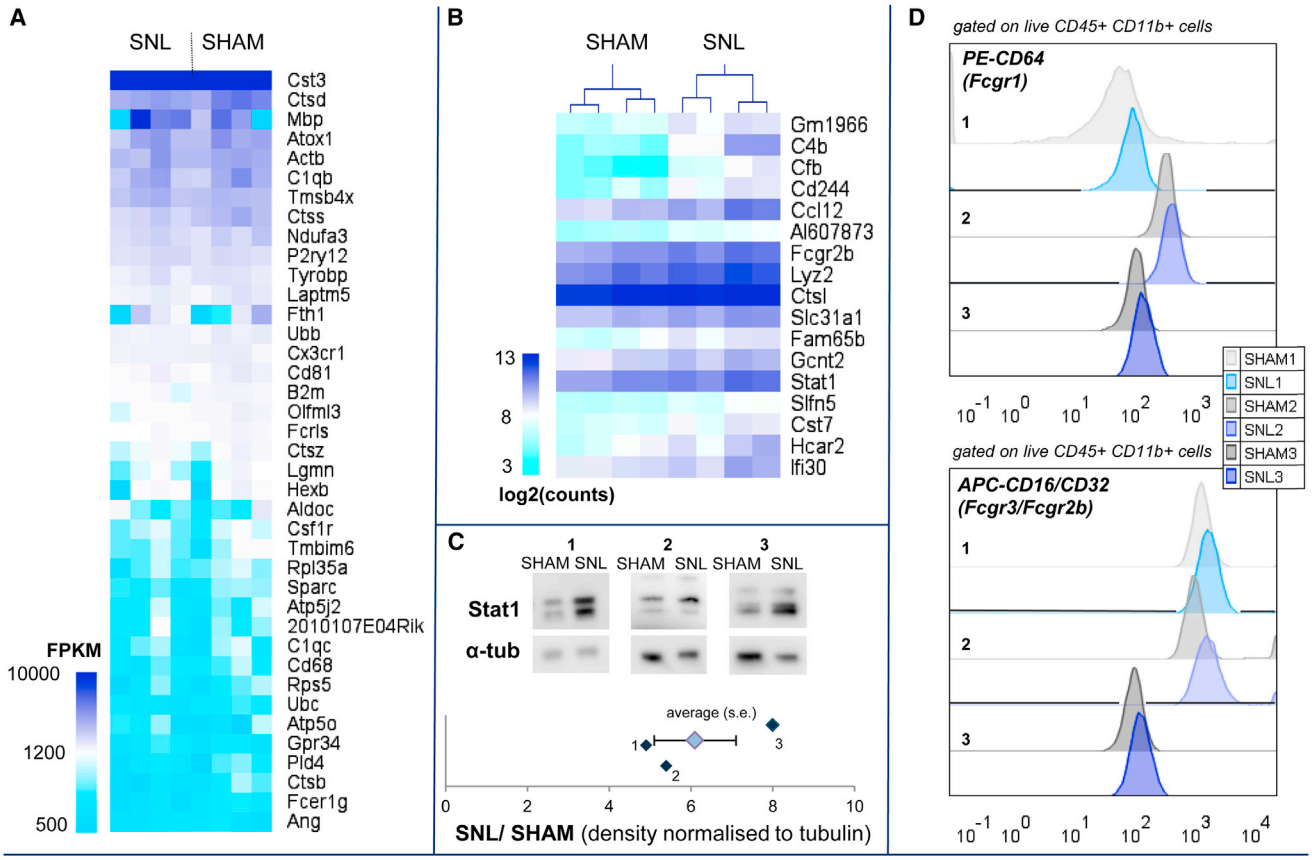

Figure 2. RNA-Seq of Isolated Microglia Reveal Cell-Type-Specific Changes in Gene Expression

(A) Top 40 expressed transcripts identified in adult spinal cord microglia in sham and SNL mice. Each column represents a biological replicate (n = 4), and individual squares represent FPKM values.

(B) Top differentially expressed genes after SNL. Squares represent log2 count data (normalized to total library size).

(C and D) Validation at protein level. (C) Significantly increased Stat1 expression was observed using western blots (one-sample t test, p = 0.034, n = 3). Plotted are band densities normalized to tubulin as a ratio of SNL/SHAM for each blot (1–3), as well as their mean fold change and SE. (D) Flow cytometry revealed increased MFIs after SNL for three Fc gamma receptors: Fcgr1 (PE-CD64, p = 0.07, n = 3), Fcgr3, and Fcgr2b (APC-CD16/CD32, p = 0.05, n = 3). An MFI ratio was calculated separately for three experiments (1–3) using constant gates between SNL and sham. Histograms are displayed after gating for live $CD45^+$, $CD11b^+$ myeloid cells. See also Figure S2 and Table S2.

et al., 2007). Using fluorescence-activated cell sorting (FACS) and ChIP-qPCR, we found no significant signal derived from the percentage of cells that are negative for CD45 and CD11b or indeed the cellular debris also contained in the preparation (Figure S1). This rules out the possibility that these factors significantly contaminate our ChIP analysis of microglia.

Genome-wide Transcriptional Profile of Isolated Spinal Cord Microglia

RNA-seq was performed on spinal microglia after SNL or sham surgery (n = 4, each n pooled from four lumbar cords). We found high expression of known microglial genes, such as cathepsins (e.g., *Ctss*), the fractalkine receptor (*Cx3cr1*), and many genes highlighted as microglial by Butovsky et al. (2014) (e.g., *Cst3*, *P2ry12*, *Fcrls*, *Csfr1*) (Figure 2A). Of the 88 microglial markers reported by Butovsky et al. (2014), 71 ranked in the top 20% of transcripts we identified by expression level (Table S1; 13,873 genes identified with cut-off set to more than three samples at fragments per kilobase of transcript per million mapped reads [FPKM] >0.3). Comparison of a larger list of 1,330 microglial genes to previously published datasets (Lavin et al., 2014; Butovsky et al., 2014) indicated a strong positive correlation in expression profiles across all three studies (Spearman's $\rho = 0.61$ and 0.66, $p < 0.001$; Figure S2).

Next, we analyzed differential gene expression between SNL and sham microglia. Using Deseq2, we identified 17 individual genes that were significantly upregulated in SNL samples at adjusted $p < 0.05$ (Figure 2B; Table S2). A network analysis of known and putative protein-protein interactions further revealed that ~50% of the genes upregulated at unadjusted $p < 0.05$ were functionally connected (107 out of 259; Figure 3). Visually, they could be grouped into four main categories: genes related to microglial activation and the subsequent immune response, genes related to interferon signaling, lysosomal genes, and genes related to mitosis and ribosomal protein synthesis. We confirmed these clusters using gene ontology (GO) enrichment

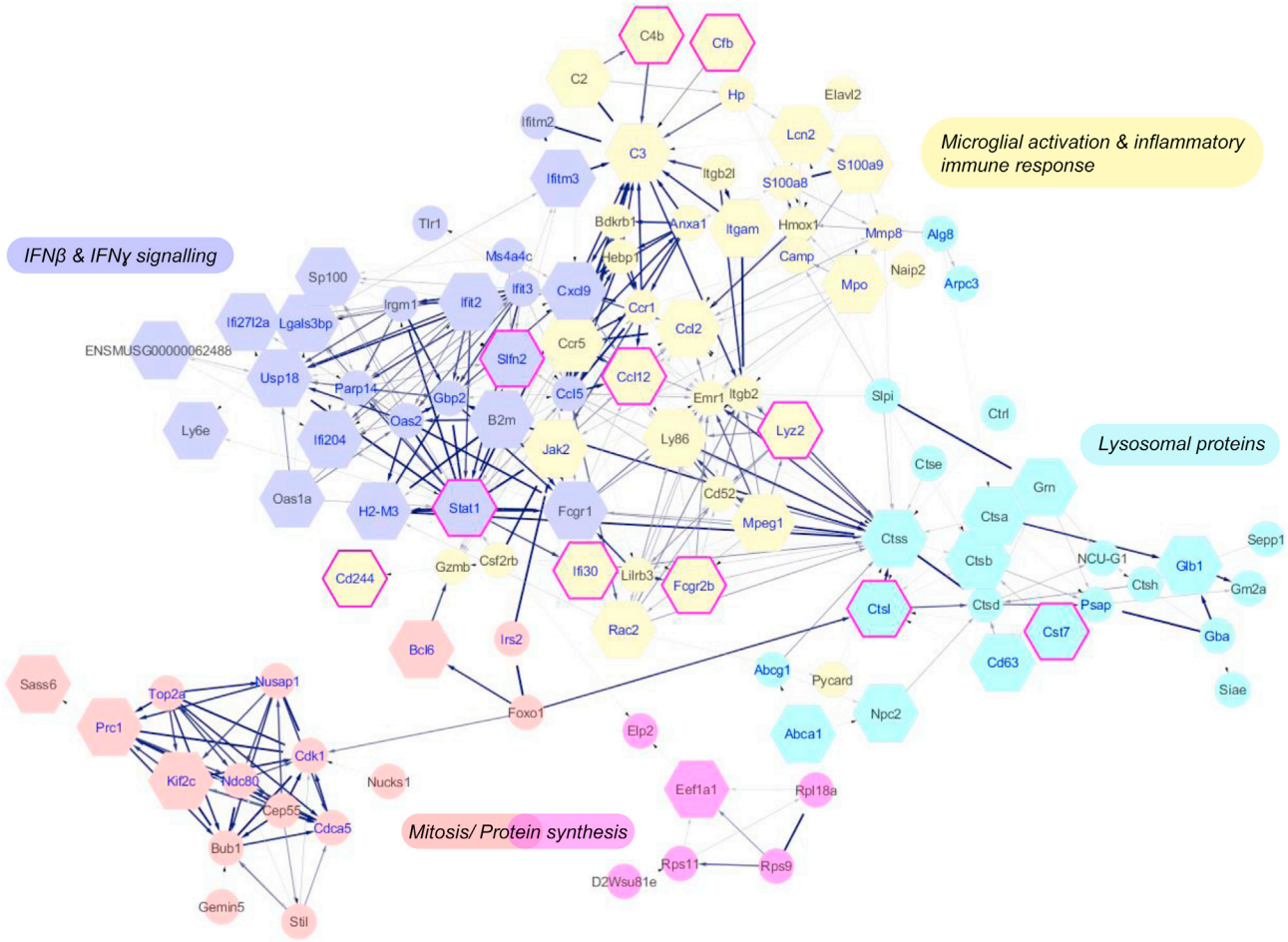

Figure 3. Network of Genes Found to be Significantly Upregulated after SNL

Network analysis revealed a set of 107 functionally interconnected genes with increased expression after nerve injury that broadly clustered into four categories. The shape of each node represents the statistical confidence at which each gene was found to be upregulated using Deseq2: unadjusted $p < 0.05$ (circles), unadjusted $p < 0.01$ (hexagons), and adjusted $p < 0.05$ (pink border). The functional information contained in this analysis reduces the chance of false positive results, but please note that they cannot be completely ruled out for individual genes, especially at $p < 0.05$ (circles).

See also Figure S3 and Table S3.

analysis, comparing the list of upregulated genes to our complete microglial gene set. Immune response terms, including interferon gamma (IFNɣ), interferon beta (IFNβ), and complement signaling, were significantly enriched (Table S3).

We did not observe any significant downregulation of genes in SNL microglia; however, when using all putatively dysregulated genes (both upregulated and downregulated at unadjusted $p < 0.05$) as seeds for a protein-protein interaction network, some downregulated genes did appear in our main network clusters as defined above (Figure S3).

Protein Level and Functional Validation of RNA-Seq Data

Injury-associated gene expression increase was accompanied by observable changes in protein levels. A western blot revealed that Stat1 was significantly elevated in Percoll-isolated microglia after SNL, mirroring our RNA-seq results (one sample t test, $p = 0.035$, $n = 3$; Figure 2C). Moreover, by measuring mean fluorescent intensity (MFI) of microglia via flow cytometry, we were able to confirm the dysregulation of Fc gamma receptors, in particular Fcgr1 (mean fold change of 1.39, one sample t test, near significant at $p = 0.07$, $n = 3$) and Fcgr2b (mean fold change of 1.48, one sample t test, $p = 0.05$, $n = 3$; Figure 2D).

To validate our network predictions, we moved into an in vitro system using an undifferentiated human monocytic cell line. Protein-protein interaction and GO analysis identified a cluster of proteins involved in interferon signaling, including Stat1 (Figure 3), suggesting that IFNɣ might be inducing some of the key microglial expression changes observed 7 days after nerve injury. Indeed, mirroring our network, stimulation of our cultured cells with IFNɣ caused a clear upregulation of *FCGR1*, *FCGR2B*, *STAT1*, *B2M*, and *CCL2*, while *FCGR3* was unaffected (Figure 4A). STAT1 did not appear to play an irreplaceable role in this process; partial knockdown of *STAT1* in monocytes had no significant effect on gene regulation

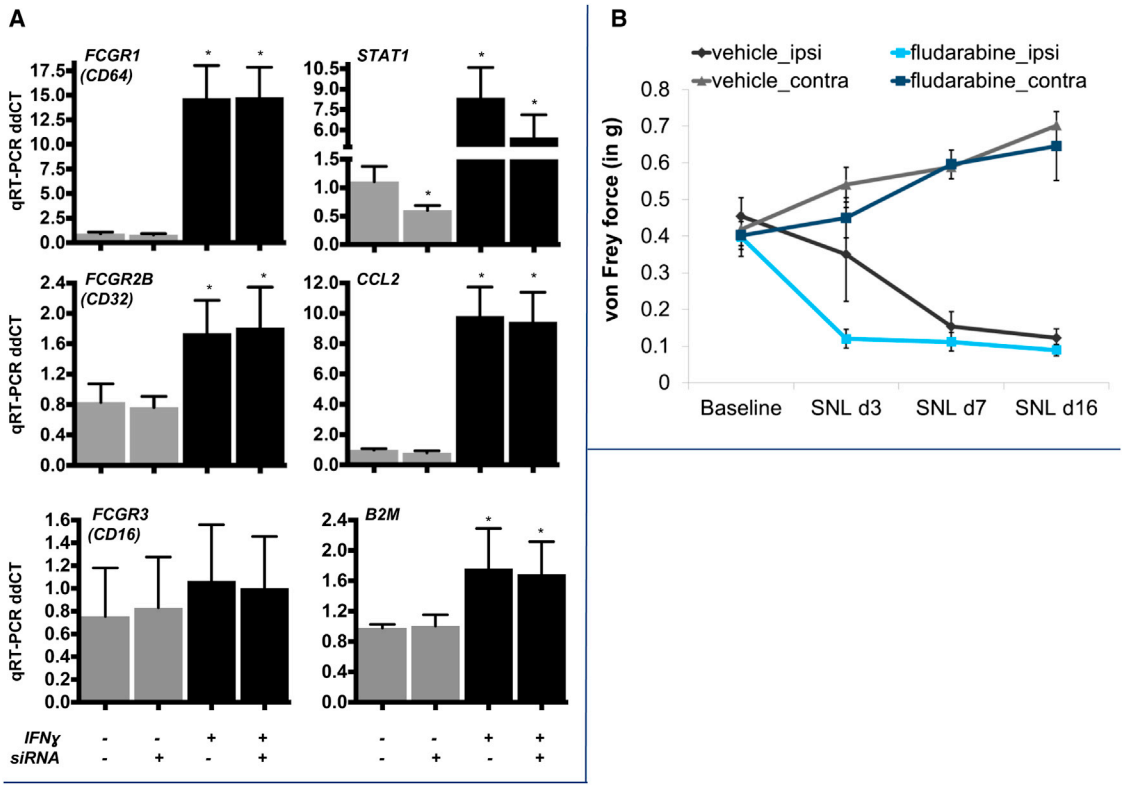

Figure 4. Functional Validation of SNL-Induced Microglial Gene Network

(A) Stimulation of the undifferentiated human monocytic cell line THP1 revealed that IFNɣ indeed regulates many of the gene expression changes identified in our RNA-seq analysis. As predicted by our network, *FCGR1*, *FCGR2B*, *STAT1*, *CCL2*, and *B2M* were significantly increased by IFNɣ, while *FCGR3* was unaffected ($p < 0.05$, ANOVA followed by LSD post hoc testing). siRNA knockdown of STAT1 did not have any effect. Plotted are ddCT values (mean + SD) after IFNɣ (+) or vehicle application (−) in the presence (+) or absence (−) of *STAT1* siRNA

(B) Inhibition of Stat1 in vivo using the inhibitor fludarabine did not affect mechanical hypersensitivity after nerve injury. A total of 30 mg/kg (SNL d3, SNLd7) or 100 mg/kg (SNL d16) of the compound was injected i.p. 1 hr before behavioral testing in mice that had undergone SNL 3 days, 7 days, or 16 days earlier. Mean withdrawal thresholds are plotted in grams with their SE.

(Figure 4A), nor did pharmacological inhibition of STAT1 in vivo have any effect on mechanical hypersensitivity after SNL in mice (Figure 4B).

Injury-Specific Alterations of Microglial Enhancer Profiles

Genome-wide H3K4me1 enrichment profiles of spinal cord microglia corresponded well to those of naive cortical microglia published recently (Lavin et al., 2014). The consensus binding profiles of sham, SNL, and cortical microglia overlapped to a significant extent, although, as expected, SNL microglia were the most divergent (Figure S4A).

A significant number of peaks were found to be differentially bound in injured microglia compared to their sham counterparts using the DiffBind algorithm with a false discovery rate (FDR) cutoff of FDR <0.1 (Figures 5A and S4B; Table S4). The regions were annotated to their nearest transcriptional start site, as well as their closest regulated gene (using Deseq2 differentially regulated genes at unadjusted $p < 0.01$). Most enhancers are likely to occur within one megabase (Mb) of their target gene (Heinz et al., 2015), therefore any regions that were >1 Mb from a dysregulated gene were disregarded. This resulted in a list of 36 putative latent enhancers and 12 putative repressed regions that emerge as a result of nerve injury. GO and pathway analyses using GREAT revealed that regions with increased H3K4me1 binding after SNL were enriched for immune and inflammatory response terms, such as regulation of lymphocyte and leukocyte proliferation and inflammation mediated by chemokines and cytokines (Figure S4C; Table S4).

Forty percent of our putative enhancer regions were within 500 kb of genes with abnormally high levels of expression after SNL (Figure S4D). Previous work on latent enhancers (Ostuni et al., 2013) indicates that 80% of binding sites emerge at this distance, and many are within 250 kb or less. In our list, 16 of 36 locations found were within 200 kb of a dysregulated gene (Figure 5B). Indeed, the closest transcriptional start sites of 9 of these 16 were genes that were found to be overexpressed after SNL. *Fam65b*, *C4b*, *Ccl12*, and *Fcgr2b* stood out in particular, as these were among the top upregulated genes identified via RNA-seq (Figure 5B).

To validate our findings, we performed ChIP-qPCR to measure H3K4me1 enrichment at selected sites in two additional, newly

Please cite this article in press as: Denk et al., Persistent Alterations in Microglial Enhancers in a Model of Chronic Pain, Cell Reports (2016), http://dx.doi.org/10.1016/j.celrep.2016.04.063

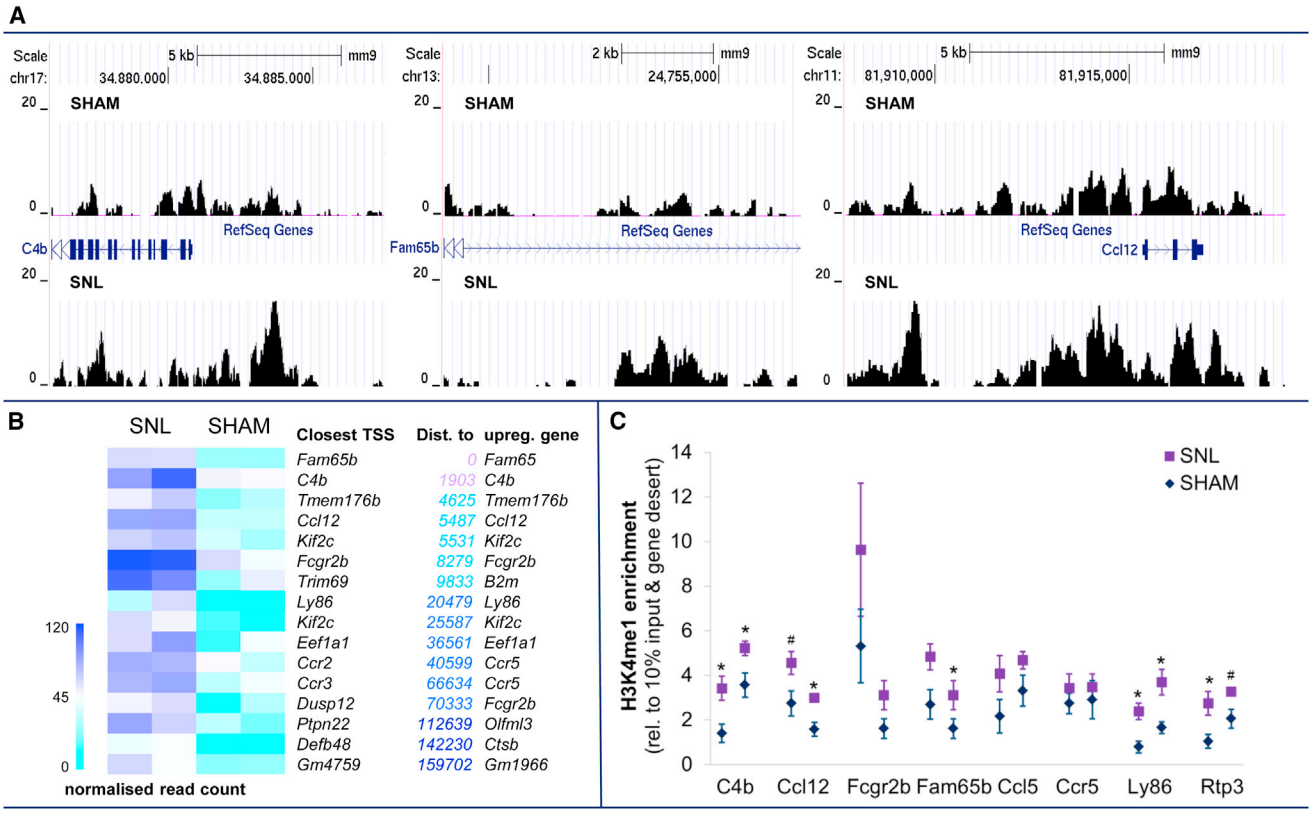

Figure 5. Microglia Enhancer Profiles Are Altered after SNL

(A) Example UCSC traces of ChIP-seq data (bigwig files of H3K4me1 normalized to 10% input). Increased binding was found at several genomic locations. Shown here are *C4b*, *Fam65b*, and *Ccl12*.

(B) Heatmap of putative latent enhancers associated with SNL. Columns are biological replicates; square boxes represent normalized read counts within a relevant peak. Displayed is the closest transcriptional start site (TSS) as well as the distance to the closest upregulated gene (in base pairs) and the identity of that gene.

(C) ChIP-qRT-PCR validation of altered binding. H3K4me1 signal is displayed relative to 10% input and a negative control gene desert region (mean and SE of two separate experiments for each region; n = 4 and n = 3 and 4, respectively). SNL resulted in consistently increased binding in seven out of the eight tested locations. *$p < 0.05$, #$p < 0.1$, heteroscedastic two-tailed t tests.

See also Figure S4 and Table S4.

generated cohorts of neuropathic mice (2 × n = 4), each with their own sham controls (n = 4, n = 3). Seven out of eight sites chosen for replication showed increased binding after SNL, five of them significantly so as measured by independent samples t tests (Figure 5C).

Persistence of Putative Latent Enhancers 28 Days after Nerve Injury

Our primary hypothesis is that latent enhancers might be a way in which injury-specific changes are encoded over long periods of time, allowing for priming of the system and ultimately the chronification of pain. To test this, we went on to perform additional analyses of our model at later time points. RNA was obtained at day 1, day 7, day 14, and day 28 after SNL. For this, we FACS-sorted microglia from dorsal ipsilateral lumbar spinal cord (Figure S5A), amplified the RNA using a multiple displacement method, and performed high-throughput qRT-PCR using TaqMan microfluidic cards. At day 7 after SNL, the 28 genes deemed to pass our expression cut-off by qPCR correlated well with our original RNA-seq (Figure 6A), serving as further validation of the transcriptomic data presented here. Moreover, it appeared that the transcriptional changes observed in microglia were transient—the vast majority of genes had reverted back to their pre-injury expression levels 28 days after SNL (Figures 6B and S5B). We also confirmed this at protein level: immunofluorescent staining revealed that Fc gamma receptor expression (CD16/C32) was still high in the ipsilateral lumbar spinal cord at day 14, but much reduced or absent in some cases at day 28 (Figure S6).

This was in stark contrast to what we found when we extracted chromatin from microglia of mice 28 days after SNL or sham surgery (n = 3). ChIP-qPCR indicated that several of the putative latent enhancer regions we identified retained their increased H3K4me1 binding levels at this late time point—up to a month after pain was first induced: *C4b*, *Ccl12*, and *Ccl5* all still showed significant enrichment (Figure 6C), and binding remained high at several other regions (*Fcgr2b*, *Fam65b*, and *Ly86*), although this was not statistically significant.

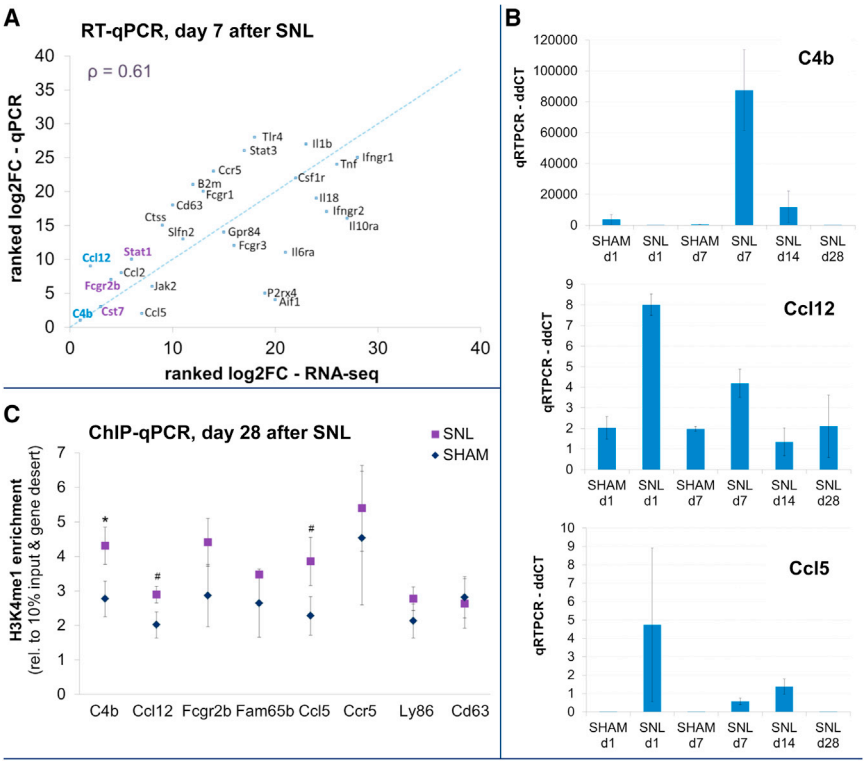

Figure 6. Microglial Enhancers Persist when Transcription Has Reverted to Baseline

(A) Further validation of RNA-seq was conducted using a TaqMan qRT-PCR array card for selected genes at different time points after injury. Microglia were isolated from lumbar ipsilateral dorsal horn and sorted using FACS. Plotted here are the ranked log2 fold changes (day 7, SNL versus sham) of 28 genes obtained from the RNA-seq (n = 4) versus those obtained from the qRT-PCR (n = 3). They were strongly correlated (Spearman's rho = 0.61, $p < 0.002$). Genes in purple were significantly dysregulated in the RNA-seq data at adjusted $p < 0.05$, genes in blue reached statistical significance via both methods.

(B) qRT-PCR at varying time points after injury demonstrated that the transcriptional changes in microglia are transient. Shown here mean ddCT values and SE for *C4b*, *Ccl12*, and *Ccl5* at day 1 (SNL d1), day 7 (SNL d7), day 14 (SNL d14), and day 28 (SNL d28) after injury compared to sham injured animals at day 1 (SHAM d1) and day 7 (SHAM d7). See Figure S5 for more plots. The changes observed for *C4b* and *Ccl12* were statistically significant (one-way ANOVA, $p = 0.006$ and $p = 0.009$, respectively).

(C) In contrast to (B), ChIP-qPCR of purified microglia at day 28 after SNL (compared to day 28 sham) demonstrated that altered H3K4me1 binding persisted at putative latent enhancers close to *C4b*, *Ccl12*, and *Ccl5* (n = 3). *$p < 0.05$, #$p < 0.1$, heteroscedastic one-tailed t test.

See also Figure S6 and Table S5.

DISCUSSION

We set out to test the hypothesis that neuropathic pain could result in injury-specific alterations to the enhancer landscape. For this, we investigated the spinal cord immune response after peripheral SNL in mice, using techniques to analyze cell composition, genome-wide transcriptional alterations, and changes to the enhancer-identifying histone mark H3K4me1.

Contrary to previous claims in the literature (Echeverry et al., 2011), we found no evidence of peripheral immune cell infiltration into the spinal cord after nerve injury. Moreover, our cell-type-specific gene expression profile revealed the unique molecular signature of the microglial inflammatory response, including some surprising findings, such as the absence of *Bdnf*. Finally, we found 16 putative enhancers that showed increased binding in microglia 7 days after nerve injury, of which nine were within 250 kb of upregulated genes. Most intriguingly, many of these potentially latent enhancer regions remained in place up to 28 days after the injury was first induced—a time point at which we could show that the vast majority of transcriptional changes had reverted back to normal.

Activity-dependent changes to enhancers have been described in the context of development (Gosselin et al., 2014), immune system function (Ostuni et al., 2013), as well as neuronal signaling (Malik et al., 2014). These range from the appearance of completely new binding regions in mature macrophages to the depolarization-induced priming of existing enhancers in neurons. Both provide a mechanism by which a stimulus could affect the response of cells in the longer term, by altering their ability to bind certain transcription factors in specific locations. In the context of nerve injury, alterations to enhancer profiles therefore present a plausible way in which maladaptive nervous system and immune responses could be "remembered," become fixed in time, and ultimately contribute to the chronification of pain.

Our results suggest the involvement of enhancers in a model of neuropathic pain and raise a multitude of intriguing questions:

1. What state are these injury-specific enhancers in? Enhancers can adopt varying conformations (inactive, primed, poised, and active), which can only be fully characterized by surveying several other chromatin marks. Are our putative enhancer regions primed for activity at day 28, ready to mount a more vigorous transcriptional response upon repeat activation?
2. How are they deposited? In macrophages, it has been shown that the deposition of new enhancer peaks requires the combined action of various TFs including Pu.1, Stat1, and Stat6 (Ostuni et al., 2013). This is of particular interest in the context of our dataset, where Stat1 expression was found to be significantly increased after SNL at both RNA and protein level.
3. Are the observed changes in enhancer profile critical for the development of chronic pain? Studying the direct

causal involvement of a specific enhancer is a complex undertaking and involves tools such as the generation of transgenic reporter lines or gene editing technologies (Kearns et al., 2015), many of which are not yet adapted for use in the CNS. Low cell numbers coupled with the requirement for high levels of cell purity further complicate study of enhancers in the neurosciences. Recent improvements to small-scale ChIP-seq (Lara-Astiaso et al., 2014) as well as the innovative method of ATAC-seq (Buenrostro et al., 2015) may help alleviate some of the methodological difficulties in this area.

It may be some time before the injury-specific enhancers we identified can be fully characterized. In the meantime, our data provide immediately useable information about spinal cord immune cell composition and microglial gene expression after injury. The dorsal horn of the spinal cord, where peripheral nociceptive afferents terminate, is a highly complex tissue with many different cell types. After spinal nerve injury, the picture is further complicated, with prior reports in the literature claiming T cell (Costigan et al., 2009) and peripheral macrophage infiltration (Zhang et al., 2007). Until recently though, the field has largely been missing the cell-type-specific tools required to examine these issues in more detail. Flow cytometry analyses are still rare in neuroscience research, and only since 2014 have there been specific antibodies available that allow the distinction between resident and infiltrating myeloid cells.

Here, we used one of these markers, the purinergic receptor P2ry12, to demonstrate that 99% of myeloid cells in the spinal cord after peripheral spinal nerve injury are resident microglia. Previous reports of macrophage infiltration after nerve injury may have arisen because it was hitherto necessary to irradiate the bone marrow in order to introduce genetically tagged peripheral monocytes. This can result in a breakdown of the blood brain barrier and artificially increase numbers of bone-marrow-derived macrophages in the CNS. We also did not observe SNL-associated changes in B cell or T cell counts, all of which were very low. Of course, we cannot exclude that T cell recruitment will start at a later stage, more than 7 days after injury.

In addition to our flow cytometry analysis, we used RNA-seq to characterize the transcriptional profile of acutely isolated microglia. We identified several clear modules of increased activity indicating that microglia are dividing and activated as expected, such as members of the alternative complement activation pathway (*C3*, *Cfb C4b*, *C2*) and their downstream receptors (*Itgam* [CD11b] and *Itgb2l* [CD18]). One intriguing hit was the upregulation of *Cd244*, which has previously been almost exclusively described in the context of natural killer (NK) and memory T cells. We and others (Butovsky et al., 2014) now find it expressed in naive microglia. Its upregulation upon injury raises the question of what its function is in these cells, as in NK cells it has both activating and inhibitory potential (McNerney et al., 2005).

Our data also highlight the importance of only a few specific chemokines and signaling pathways and may therefore help direct efforts to find pharmacological targets. Cell-type-specific RNA-seq confirmed a role for Ccl2, its mouse ortholog Ccl12, and Ccl5, which have already been identified in previous literature (Old and Malcangio, 2012). Additionally, a network analysis identified IFNɣ as a potentially important upstream mediator of SNL-induced gene regulation in microglia—a result that we were able to validate functionally in an undifferentiated human monocyte cell line. IFNɣ appears to regulate the expression of *Stat1*, *Ccl2*, and fragment-crystallizable gamma ɣ receptors (FcɣRs). FcɣRIIb (*Fcgr2b*, CD32b) expression was increased in our RNA-seq data, as well as in subsequent validation experiments examining both RNA and protein. CD16 (*Fcgr3*) was not found to be regulated, neither in microglia nor IFNɣ-stimulated monocytes. The role of the activating receptor FcɣRI (*Fcgr1*, CD64) was less clear: it was induced by IFNɣ in monocytes, and there was a near-significant increase in microglia after SNL at protein, but not transcript level. FcɣRs are the main receptors for immunoglobulins, and their balanced response is crucial for a well-adjusted innate immune response (Nimmerjahn and Ravetch, 2008). Shifts in FcɣR function toward too much or too little activation have been linked to a variety of diseases, including those with a chronic pain component, such as rheumatoid arthritis and inflammatory bowel syndrome (Franke et al., 2016). At least in other cell types, like neutrophils, FcɣRs, and in particular FcɣRIIb, can also directly impact complement-induced responses (Karsten et al., 2012).

Spinal microglia release a host of cytokines and other mediators as a result of peripheral neuropathic injury that negatively affect neuronal function. Our network suggests that this response is driven by the delicate interplay of a few pro-inflammatory and immunomodulatory drivers: complements, FcɣRs, and INFs, in particular IFNɣ.

Finally, qRT-PCR follow up of our RNA-seq study clearly highlighted the transient nature of the gene expression changes that take place in microglia. One month after injury, most have reverted back to their pre-injury expression levels. In contrast, several of our putative latent enhancer regions were maintained in microglia at this time—a most intriguing observation that suggests that some of the more persistent consequences of nerve injury may be hidden in the epigenome.

In summary, our study revealed several features that characterize the spinal cord microglial response in a model of persistent pain. We have shown that it is primarily dependent on resident microglia. We have presented a detailed molecular view of the ensuing microglial-specific gene expression changes. Finally, we have provided evidence for persistent injury-specific alterations of the microglial enhancer landscape. We expect that our findings will aid future research by providing several genome-wide datasets, and we hope that they will ultimately aid patients by deepening our understanding of why the nervous system is chronically dysregulated in neuropathic pain.

EXPERIMENTAL PROCEDURES

Animal Surgeries and Behavior

All work conformed to United Kingdom Home Office legislation (Scientific Procedures Act 1986). Male C57BL/6 mice were used throughout the study. SNL surgery was performed by tying a 5.0 Vicryl suture through the sciatic nerve. Corresponding sham surgery exposed the nerve, but left it intact. Mechanical hypersensitivity was assessed with von Frey hairs using the up-down method (Bonin et al., 2014). Fludarabine (S1229, Selleck Chemicals) or vehicle (0.9% saline) was delivered intraperitoneally (i.p.) at a dose of 30 mg/kg (d3 and d7) and 100 mg/kg (d16) 1–2 hr before the behavioral assessment. The

compound is known to cross the blood brain barrier (Jensen et al., 2012), and our dosing regime was based on previous literature (Chun et al., 1991; Frank et al., 1999). The experimenter was blind to the treatment.

Microglial Isolation

Seven days after SNL or sham surgery, mice were sacrificed by overdose of anesthetic and perfusion with ice-cold PBS. The spinal cord was extracted using hydroextrusion, dounce homogenized in 0.2% BSA in Hank's balanced salt solution (HBSS), and microglia isolated using a Percoll density gradient (37% versus 70%). Cells were counted on a hemocytometer and further processed for RNA extraction, chromatin extraction, flow cytometry, or FACS. For all experiments, two to eight segments of mouse cord were extracted on a given day (2–4× sham and 2–4× SNL) and pooled onto two Percoll gradients to make up one n for each group. For ChIP-seq, ~20,000 cells were removed to allow cytometry analysis of each sample before processing the remainder for chromatin extraction.

Flow Cytometry

Microglia were centrifuged (200 × *g* for 3 min at 4°C) and stained with Live/Dead fixable yellow dye (L-34959, Life Technologies) in HBSS for 30 min on ice in the dark. After a second spin, cells were stained in FACS buffer (0.4% BSA, 15 mM HEPES, 2 mM EDTA in HBSS) with rat anti-P2RY12 antibody (a gift from Dr. Oleg Butovsky) for 20 min on ice in the dark. After a wash in FACS buffer, an APC-conjugated anti-rabbit secondary antibody was used (A10931, Life Technologies). Cells were then washed once more, before being incubated with the remaining directly conjugated primary antibodies, all raised in rat and obtained from Biolegend: Alexa-Fluor-488-CD45 (103121), Pacific Blue-CD11b (101223), PE-Ly6C (128007), PE/Cy7-Ly6G (127617), Brilliant Violet-CD3 (100237), and APC/Cy7-CD19 (115529). The stained microglia were fixed for 5 min in 4% paraformaldehyde (PFA) and kept in FACS buffer until flow cytometry on a BD SORP Fortessa at the National Institute for Health Research (NIHR) Biomedical Research Centre (BRC) flow core facility at King's College London. The following controls were employed to ensure accurate compensation: unstained microglial cells, single-staining controls (cells for live/dead, BD Comp beads [BD Biosciences, 552845] for all other colors), and cells in which the primary anti-mouse P2RY12 antibody was omitted to control for potential background arising from the APC anti-rabbit secondary antibody. For any data analysis, gating was kept constant across conditions. Mean fluorescent intensity (MFI) analysis was performed after staining cells first with Live/Dead fixable yellow dye and subsequently with the following primary antibodies (all from Biolegend): Alexa-Fluor-488-CD45 (103121), Pacific Blue-CD11b (101223), PE-CD64 (139303), and APC-CD16/C32(101325). Experiments were conducted in biological triplicate and analyzed in a within-experiment manner, whereby all gates were kept the same between a sham and SNL sample pair. After the MFI was determined, a ratio of SNL/sham was generated, which was then compared across experiments using a one-sample t test with a test value of 1.

FACS

Microglia were centrifuged and stained with primary antibodies in FACS buffer for 20 min on ice in the dark (Pacific Blue-CD45, 103125, APC/Cy7-CD11b, 101225, Biolegend). DAPI was used as a viability dye. Unstained cells and single staining controls were employed as described above. Microglia were purified on a BD FACS Aria II Cell Sorter at the NIHR BRC flow core facility at King's College London and collected either into RLT buffer for RNA extraction or in FACS buffer for chromatin extraction.

Chromatin Extraction

Cells were shaken in 1% formaldehyde in FACS buffer for 5 min at room temperature and the fixation reaction terminated by the addition of 0.125 M glycine. After a wash with PBS and proteinase inhibitors, microglia were pelleted and stored at −80°C until lysis.

ChIP

Samples were generated in pairs of SNL and sham (each a pool from 4× mice) and stored at −80°C. Once a full experimental set was obtained (n = 4 pairs for sequencing; n = 8, n = 7, n = 6 pairs for three separate qRT-PCR studies), samples were lysed and pooled once more to obtain sufficient material for downstream analysis (final n = 2 for sequencing, n = 4, n = 3 and n = 3 for 3× qRT-PCR studies). Cells for ChIP-seq and the first qPCR validation cohort (Figure 5C) were derived from the entire lumbar enlargement, while cells for the other two validation cohorts (Figures 5C and 6C) were derived from ipsilateral lumbar enlargements. Chromatin was sheared in a Diagenode bath sonicator with eight repeats of 5-min cycles (30 s on, 30 s off). Immunoprecipitation was performed with an antibody against H3K4me1 (ab8895, lot GR159018-1, Abcam) using the Diagenode True MicroChIP kit following manufacturer's instructions (AB-002-0016, Diagenode). Before precipitation, 10% of the input chromatin was removed and decrosslinked. Two microliters were used to check DNA concentrations on a Qubit fluorometer, as well as shear sizes on an Agilent2100 Bioanalyzer DNA High Sensitivity ChIP. The remainder was used for sequencing or qRT-PCR controls.

ChIP-qPCR

DNA obtained from ChIP was amplified on a Roche LightCycler480 using SYBR green mastermix (04707516001, Roche) and standard run parameters. Each sample was normalized to its own 10% input control and negative control primer signal to account for individual differences in initial chromatin amount and noise levels. Standard and melt curves were generated for each run to ensure adequate primer efficiency and selectivity. See Table S5 for primer sequences.

RNA Extraction

For RNA-seq, lumbar cords and Percoll isolation was used, in order to allow direct comparison to our ChIP-seq dataset. For qRT-PCR validation of our RNA-seq data, we FACS-sorted the microglia as described above, using only dorsal ipsilateral lumbar segments. In all cases, cells were lysed in RLT buffer with beta-mercaptoethanol, and RNA was extracted using a QIAGEN RNeasy Micro Kit (74004) following the manufacturer's protocol with some minor modifications. RNA quality and quantity was assessed on an Agilent Bioanalyzer Pico chip. For sequencing, RNA was then shipped to Oxford for library preparation (see below). For qRT-PCR, RNA was amplified and converted to cDNA using the QIAGEN Repli-G single cell WTA kit according to the handbook instructions.

qRT-PCR

cDNA was quantified using a Qubit ssDNA assay kit, diluted to 2 ng/μl and loaded onto TaqMan microfluidic PCR array cards. We used the ddCT method, normalizing each sample to the average of several housekeeping genes and the same naive microglial pool. See Table S5 for the TaqMan probes used (Life Technologies).

Protein Extraction and Western Blotting

Isolated microglia were lysed in 0.2% SDS in water with proteinase and phosphatase inhibitors. The samples were reduced in 5× Laemmli buffer (50 mM Tris, ph 6.8, 2% SDS, 10% glycerol, 0.1 M DTT, beta-mercaptoethanol) and run on NuPage Novex 4%–12% Bis-Tris gradient gels (Life Technologies). After transfer onto a polyvinylidene fluoride (PVDF) membrane, staining was performed using the following antibodies: STAT1 (9172, Cell Signaling), alpha-tubulin (T9026, Sigma Aldrich), and ECL anti-rabbit and anti-mouse secondary antibodies (10794347 and 10094724, Fisher Scientific). The signal was exposed using an ECL prime kit (RPN2232, Amersham) and visualized on a UVP Biospectrum 810 Imaging System.

In Vitro Experiments

Confluent (70%–80%) THP1 cells (P3, P5, P6) were incubated for 5 hr in serum-free DMEM, supplemented with small interfering RNA (siRNA) transfection reagent (jetPEI, Polyplus) pre-mixed with either scrambled (AM4611, Ambion) or *STAT1* (s279, Ambion)-validated siRNA (20 pM). Subsequently, the culture medium was replaced with fresh DMEM and 1.5% FCS, and cells were rested overnight. The transfection was repeated the following day, and the cells were kept for another 24 hr in fresh culture medium. Prior to stimulation, siRNA-transfected cells were serum-starved in plain DMEM for 3 hr. Finally, cells were stimulated with IFNγ (40 ng/ml) for 6 hr to determine acute regulation of transcripts and avoid potential effects from cytokines synthesized and secreted by THP1

Please cite this article in press as: Denk et al., Persistent Alterations in Microglial Enhancers in a Model of Chronic Pain, Cell Reports (2016), http://dx.doi.org/10.1016/j.celrep.2016.04.063

cells following stimulation with IFNγ. Cells were lysed in TRK lysis buffer (Omega Bio-Tek), RNA was extracted using the EZNA total RNA kit I (Omega Bio-Tek) and converted to cDNA using the high capacity RNA-to-cDNA kit (Applied Biosystems). qRT-PCR was performed on a Roche LightCycler480 using the following pre-validated TaqMan primer/probe mixes (Applied Biosystems): *FCGR2B* (Hs01634996_s1), *FCGR1* (Hs00417598_m1), *STAT1* (Hs01013996_m1), and *CCL2* (Hs00234140_m1). *GAPDH* was used as housekeeper for ddCT calculations.

Immunohistochemistry

Mice were perfused with 0.2 M PB followed by 4% paraformaldehyde, and lumbar spinal cords were dissected, cryoprotected in 20% sucrose, and cut on a cryostat in 20-μm sections. Cords were collected from two separate time points (day 14 and day 28 after nerve injury) from both SNL and SHAM mice (n = 3 per SNL time point, n = 2 per sham time point). The tissue was stained by blocking in 10% BSA for 1 hr, followed by incubation with the primary antibodies overnight (Iba1, 019-19741, Wako; CD16/CD32, 553142, BD Biosciences; PE-CD64, 139303, Biolegend). After several PBS washes, the secondary antibodies were added for 2 hr (anti-rat Alexa488, anti-rabbit Alexa594), and the slides mounted after more washes with hard-set medium containing DAPI (Vector Labs). Images were taken on a Zeiss confocal microscope.

Sequencing

Sequencing was performed by the High Throughput Genomics Group at the Wellcome Trust Centre for Human Genetics (Oxford University). RNA libraries were prepared using a SMARTer Ultra Low Input HV kit (634820, Clontech). ChIP-seq libraries were prepared on the automated Wafergen's Apollo Prep system using a PrepX ILMN 32i 96 sample library kit (400076, Wafergen Biosystems). All RNA libraries and all ChIP libraries were prepared together to avoid batch effects. In both cases, custom adaptor and barcode tags were used (5′-P-GATCGGAAGAGCGGTTCAGCAGGAATGCCGAG, 5′-ACACTCTTTCCCTACACGACGCTCTTCCGATCT). Samples were amplified (18 cycles for ChIP, 13 cycles for RNA) and multiplexed in replicate flow cells on an Illumina HiSeq2500 platform to yield 50-bp paired-end reads at a depth of at least 40 M (ChIP-seq) or 20 M (RNA-seq).

RNA-Seq Data Analysis

Samples (n = 4) were sequenced, each consisting of microglia obtained from a pool of four sham or four SNL lumbar cords. Quality control, alignment, and expression level analyses were performed on the Galaxy server (Blankenberg et al., 2010; Giardine et al., 2005; Goecks et al., 2010), while differential expression was performed using Bio-Linux 7 (Field et al., 2006). FastQC (http://www.bioinformatics.babraham.ac.uk/projects/fastqc/) showed that base calls were of high quality across the full length of the reads. Alignments were performed to mouse mm9 using tophat2 (Kim et al., 2013) with a maximum of two multiple alignments permitted (-g 2). Alignment rates were between 74% and 88% (average 85.26%). The cufflinks algorithm (Trapnell et al., 2010) was run to determine FPKM values (multiple read and effective length corrections were used, and fragments of <150 bp in size were excluded to avoid unreliable quantification for genes significantly shorter than the average fragment size). Genes with an FPKM of at least 0.3 in more than three samples within a group were considered expressed. For differential expression, count data were generated using HT-seq (Anders et al., 2015) and fed into the Deseq2 algorithm (Love et al., 2014) in R. Network analyses were conducted using STRING (Szklarczyk et al., 2015), allowing all active prediction methods at medium confidence (default). Only nodes connected to the main network cluster were included in the final network. Gene ontology was determined in GOrilla (Eden et al., 2009): lists of upregulated or downregulated genes at unadjusted $p < 0.05$ (Deseq2) were compared to a background list of all microglial genes (cufflinks, FPKM cutoff of 0.3 in at least three samples). For visualizations, heatmaps were generated using the MultiExperiment Viewer software (MeV) and networks edited in Cytoscape.

ChIP-Seq Data Analysis

As above, FastQC and alignments were performed on the Galaxy server (Blankenberg et al., 2010; Giardine et al., 2005; Goecks et al., 2010). Reads were aligned to the mm9 genome using bowtie2 with the following parameters: -n 0, -e 40, -m 1, -best. Various additional quality controls were performed: CHANCE (Diaz et al., 2012), phantompeaks (Landt et al., 2012), and fraction of reads in peaks analysis. Peak finding was performed using MACS1.4.2 with default parameters (Zhang et al., 2008), and differential binding was tested with the DiffBind package in R (Ross-Innes et al., 2012).

ACCESSION NUMBERS

The accession number for the datasets reported in this paper is Gene Expression Omnibus (Edgar et al., 2002): GSE71136 (with subseries GSE71133 for RNA-seq and GSE71134 for ChIP-seq).

SUPPLEMENTAL INFORMATION

Supplemental Information includes six figures and five tables and can be found with this article online at http://dx.doi.org/10.1016/j.celrep.2016.04.063.

AUTHOR CONTRIBUTIONS

F.D., M.C., and S.B.M. designed the experiments and wrote the MS. F.D. carried out most of the experiments and the data analysis. M.C. carried out parts of the RNA collection and data analysis. A.D. carried out the in vitro mechanistic studies on monocytes. D.L. conducted the behavioral testing and carried out the immunohistochemical experiments.

ACKNOWLEDGMENTS

This research was funded by the Wellcome Trust (097903/Z/11/Z) and by an MRC ERA-NET Neuron grant (MR/M501785/1). We thank Dr. Oleg Butovsky and his team at Harvard University for his generous gift of P2RY12 antibody and for sharing his microglial extraction protocols. We would also like to thank the High-Throughput Genomics Group at the Wellcome Trust Centre for Human Genetics (funded by Wellcome Trust grant 090532/Z/09/Z) for the generation of the sequencing data. The work was further supported by the National Institute for Health Research (NIHR) Biomedical Research Centre based at Guy's and St. Thomas' NHS Foundation Trust and King's College London. The views expressed are those of the author(s) and not necessarily those of the NHS, the NIHR, or the Department of Health.

Received: July 20, 2015
Revised: November 25, 2015
Accepted: April 17, 2016
Published: May 12, 2016

REFERENCES

Anders, S., Pyl, P.T., and Huber, W. (2015). HTSeq–a Python framework to work with high-throughput sequencing data. Bioinformatics *31*, 166–169.

Blankenberg, D., Von Kuster, G., Coraor, N., Ananda, G., Lazarus, R., Mangan, M., Nekrutenko, A., and Taylor, J. (2010). Galaxy: a web-based genome analysis tool for experimentalists. Curr. Protoc. Mol. Biol. *Chapter 19*, Unit 19.10.1–21.

Bonin, R.P., Bories, C., and De Koninck, Y. (2014). A simplified up-down method (SUDO) for measuring mechanical nociception in rodents using von Frey filaments. Mol. Pain *10*, 26.

Buenrostro, J.D., Wu, B., Chang, H.Y., and Greenleaf, W.J. (2015). ATAC-seq: a method for assaying chromatin accessibility genome-wide. Curr. Protoc. Mol. Biol. *109*, 21.29.1–9.

Butovsky, O., Jedrychowski, M.P., Moore, C.S., Cialic, R., Lanser, A.J., Gabriely, G., Koeglsperger, T., Dake, B., Wu, P.M., Doykan, C.E., et al. (2014). Identification of a unique TGF-β-dependent molecular and functional signature in microglia. Nat. Neurosci. *17*, 131–143.

Chee, P.Y., and Dahl, J.L. (1978). Measurement of protein turnover in rat brain. J. Neurochem. *30*, 1485–1493.

Chun, H.G., Leyland-Jones, B., and Cheson, B.D. (1991). Fludarabine phosphate: a synthetic purine antimetabolite with significant activity against lymphoid malignancies. J. Clin. Oncol. *9*, 175–188.

Costigan, M., Moss, A., Latremoliere, A., Johnston, C., Verma-Gandhu, M., Herbert, T.A., Barrett, L., Brenner, G.J., Vardeh, D., Woolf, C.J., and Fitzgerald, M. (2009). T-cell infiltration and signaling in the adult dorsal spinal cord is a major contributor to neuropathic pain-like hypersensitivity. J. Neurosci. *29*, 14415–14422.

Diaz, A., Nellore, A., and Song, J.S. (2012). CHANCE: comprehensive software for quality control and validation of ChIP-seq data. Genome Biol. *13*, R98.

Echeverry, S., Shi, X.Q., Rivest, S., and Zhang, J. (2011). Peripheral nerve injury alters blood-spinal cord barrier functional and molecular integrity through a selective inflammatory pathway. J. Neurosci. *31*, 10819–10828.

Eden, E., Navon, R., Steinfeld, I., Lipson, D., and Yakhini, Z. (2009). GOrilla: a tool for discovery and visualization of enriched GO terms in ranked gene lists. BMC Bioinformatics *10*, 48.

Edgar, R., Domrachev, M., and Lash, A.E. (2002). Gene Expression Omnibus: NCBI gene expression and hybridization array data repository. Nucleic Acids Res. *30*, 207–210.

Field, D., Tiwari, B., Booth, T., Houten, S., Swan, D., Bertrand, N., and Thurston, M. (2006). Open software for biologists: from famine to feast. Nat. Biotechnol. *24*, 801–803.

Frank, D.A., Mahajan, S., and Ritz, J. (1999). Fludarabine-induced immunosuppression is associated with inhibition of STAT1 signaling. Nat. Med. *5*, 444–447.

Franke, L., El Bannoudi, H., Jansen, D.T., Kok, K., Trynka, G., Diogo, D., Swertz, M., Fransen, K., Knevel, R., Gutierrez-Achury, J., et al. (2016). Association analysis of copy numbers of FC-gamma receptor genes for rheumatoid arthritis and other immune-mediated phenotypes. Eur. J. Hum. Genet. *24*, 263–270.

Giardine, B., Riemer, C., Hardison, R.C., Burhans, R., Elnitski, L., Shah, P., Zhang, Y., Blankenberg, D., Albert, I., Taylor, J., et al. (2005). Galaxy: a platform for interactive large-scale genome analysis. Genome Res. *15*, 1451–1455.

Goecks, J., Nekrutenko, A., and Taylor, J.; Galaxy Team (2010). Galaxy: a comprehensive approach for supporting accessible, reproducible, and transparent computational research in the life sciences. Genome Biol. *11*, R86.

Gosselin, D., Link, V.M., Romanoski, C.E., Fonseca, G.J., Eichenfield, D.Z., Spann, N.J., Stender, J.D., Chun, H.B., Garner, H., Geissmann, F., and Glass, C.K. (2014). Environment drives selection and function of enhancers controlling tissue-specific macrophage identities. Cell *159*, 1327–1340.

Heintzman, N.D., Stuart, R.K., Hon, G., Fu, Y., Ching, C.W., Hawkins, R.D., Barrera, L.O., Van Calcar, S., Qu, C., Ching, K.A., et al. (2007). Distinct and predictive chromatin signatures of transcriptional promoters and enhancers in the human genome. Nat. Genet. *39*, 311–318.

Heinz, S., Romanoski, C.E., Benner, C., and Glass, C.K. (2015). The selection and function of cell type-specific enhancers. Nat. Rev. Mol. Cell Biol. *16*, 144–154.

Jensen, K., Johnson, L.A., Jacobson, P.A., Kachler, S., Kirstein, M.N., Lamba, J., and Klotz, K.N. (2012). Cytotoxic purine nucleoside analogues bind to A1, A2A, and A3 adenosine receptors. Naunyn Schmiedebergs Arch. Pharmacol. *385*, 519–525.

Kaikkonen, M.U., Spann, N.J., Heinz, S., Romanoski, C.E., Allison, K.A., Stender, J.D., Chun, H.B., Tough, D.F., Prinjha, R.K., Benner, C., and Glass, C.K. (2013). Remodeling of the enhancer landscape during macrophage activation is coupled to enhancer transcription. Mol. Cell *51*, 310–325.

Karsten, C.M., Pandey, M.K., Figge, J., Kilchenstein, R., Taylor, P.R., Rosas, M., McDonald, J.U., Orr, S.J., Berger, M., Petzold, D., et al. (2012). Anti-inflammatory activity of IgG1 mediated by Fc galactosylation and association of FcγRIIB and dectin-1. Nat. Med. *18*, 1401–1406.

Kearns, N.A., Pham, H., Tabak, B., Genga, R.M., Silverstein, N.J., Garber, M., and Maehr, R. (2015). Functional annotation of native enhancers with a Cas9-histone demethylase fusion. Nat. Methods *12*, 401–403.

Kim, D., Pertea, G., Trapnell, C., Pimentel, H., Kelley, R., and Salzberg, S.L. (2013). TopHat2: accurate alignment of transcriptomes in the presence of insertions, deletions and gene fusions. Genome Biol. *14*, R36.

Landt, S.G., Marinov, G.K., Kundaje, A., Kheradpour, P., Pauli, F., Batzoglou, S., Bernstein, B.E., Bickel, P., Brown, J.B., Cayting, P., et al. (2012). ChIP-seq guidelines and practices of the ENCODE and modENCODE consortia. Genome Res. *22*, 1813–1831.

Lara-Astiaso, D., Weiner, A., Lorenzo-Vivas, E., Zaretsky, I., Jaitin, D.A., David, E., Keren-Shaul, H., Mildner, A., Winter, D., Jung, S., et al. (2014). Immunogenetics. Chromatin state dynamics during blood formation. Science *345*, 943–949.

Lavin, Y., Winter, D., Blecher-Gonen, R., David, E., Keren-Shaul, H., Merad, M., Jung, S., and Amit, I. (2014). Tissue-resident macrophage enhancer landscapes are shaped by the local microenvironment. Cell *159*, 1312–1326.

Loggia, M.L., Chonde, D.B., Akeju, O., Arabasz, G., Catana, C., Edwards, R.R., Hill, E., Hsu, S., Izquierdo-Garcia, D., Ji, R.R., et al. (2015). Evidence for brain glial activation in chronic pain patients. Brain *138*, 604–615.

Love, M.I., Huber, W., and Anders, S. (2014). Moderated estimation of fold change and dispersion for RNA-seq data with DESeq2. Genome Biol. *15*, 550.

Malik, A.N., Vierbuchen, T., Hemberg, M., Rubin, A.A., Ling, E., Couch, C.H., Stroud, H., Spiegel, I., Farh, K.K., Harmin, D.A., and Greenberg, M.E. (2014). Genome-wide identification and characterization of functional neuronal activity-dependent enhancers. Nat. Neurosci. *17*, 1330–1339.

McMahon, S.B., La Russa, F., and Bennett, D.L. (2015). Crosstalk between the nociceptive and immune systems in host defence and disease. Nat. Rev. Neurosci. *16*, 389–402.

McNerney, M.E., Lee, K.M., and Kumar, V. (2005). 2B4 (CD244) is a non-MHC binding receptor with multiple functions on natural killer cells and CD8+ T cells. Mol. Immunol. *42*, 489–494.

Nimmerjahn, F., and Ravetch, J.V. (2008). Fcgamma receptors as regulators of immune responses. Nat. Rev. Immunol. *8*, 34–47.

Old, E.A., and Malcangio, M. (2012). Chemokine mediated neuron-glia communication and aberrant signalling in neuropathic pain states. Curr. Opin. Pharmacol. *12*, 67–73.

Ostuni, R., Piccolo, V., Barozzi, I., Polletti, S., Termanini, A., Bonifacio, S., Curina, A., Prosperini, E., Ghisletti, S., and Natoli, G. (2013). Latent enhancers activated by stimulation in differentiated cells. Cell *152*, 157–171.

Quintin, J., Cheng, S.C., van der Meer, J.W., and Netea, M.G. (2014). Innate immune memory: towards a better understanding of host defense mechanisms. Curr. Opin. Immunol. *29*, 1–7.

Ross-Innes, C.S., Stark, R., Teschendorff, A.E., Holmes, K.A., Ali, H.R., Dunning, M.J., Brown, G.D., Gojis, O., Ellis, I.O., Green, A.R., et al. (2012). Differential oestrogen receptor binding is associated with clinical outcome in breast cancer. Nature *481*, 389–393.

Szklarczyk, D., Franceschini, A., Wyder, S., Forslund, K., Heller, D., Huerta-Cepas, J., Simonovic, M., Roth, A., Santos, A., Tsafou, K.P., et al. (2015). STRING v10: protein-protein interaction networks, integrated over the tree of life. Nucleic Acids Res. *43*, D447–D452.

Trapnell, C., Williams, B.A., Pertea, G., Mortazavi, A., Kwan, G., van Baren, M.J., Salzberg, S.L., Wold, B.J., and Pachter, L. (2010). Transcript assembly and quantification by RNA-Seq reveals unannotated transcripts and isoform switching during cell differentiation. Nat. Biotechnol. *28*, 511–515.

Zhang, J., Shi, X.Q., Echeverry, S., Mogil, J.S., De Koninck, Y., and Rivest, S. (2007). Expression of CCR2 in both resident and bone marrow-derived microglia plays a critical role in neuropathic pain. J. Neurosci. *27*, 12396–12406.

Zhang, Y., Liu, T., Meyer, C.A., Eeckhoute, J., Johnson, D.S., Bernstein, B.E., Nusbaum, C., Myers, R.M., Brown, M., Li, W., and Liu, X.S. (2008). Model-based analysis of ChIP-Seq (MACS). Genome Biol. *9*, R137.